IEEE Access
Multidisciplinary | Rapid Review | Open Access Journal

Received 4 January 2025, accepted 11 January 2025, date of publication 15 January 2025, date of current version 14 February 2025.

Digital Object Identifier 10.1109/ACCESS.2025.3529914

RESEARCH ARTICLE

Multi-Class Diagnosis of Neurodegenerative Diseases Using Effective Deep Learning Models With Modified DenseNet-169 and Enhanced DeepLabV3+

SRINIVAS KATKAM[1], V. PREMA TULASI[2], B. DHANALAXMI[3], AND J. HARIKIRAN[4]

[1]Department of Computer Science and Engineering, Geethanjali College of Engineering and Technology, Cheeryal, Telangana 501301, India
[2]Department of Computer Science and Engineering (Data Science), CMR Technical Campus (Autonomous), Hyderabad, Telangana 501401, India
[3]Department of Computer Science and Engineering - Cyber Security, Geethanjali College of Engineering and Technology, Hyderabad, Telangana 501301, India
[4]School of Computer Science and Engineering, VIT-AP University, Amaravati, Andhra Pradesh 522237, India

Corresponding author: J. Harikiran (harikiran.j@vitap.ac.in)

ABSTRACT Early detection lowers the death rate and allows for prompt treatment of the exhausted individual with neurodegenerative diseases. Most existing classification studies can either not generate probabilistic predictions or consider uncertainty, or do not reflect medical practice, where patients may have unusual variations, comorbidities, or early stages of the disease. This research proposes a novel method for classifying patients and healthy individuals from other distinctive neurodegenerative diseases that consider ambiguity and spatial information. Based on improved deep learning models, we presented a multi-class neurodegenerative disease classification in this research that accurately conducts multi-class or three-class classifications. First, we use various pre-processing methods to make the data suitable for analysis, such as noise reduction, contrast improvement, and data augmentation. The CapsNet model is then used to extract the images' valuable features. Then, the multi-class classifications of neurodegenerative diseases are classified using the Modified DenseNet-169 model. After classification, the accurate delineation of disease regions is effectively segmented using the Enhanced DeepLabV3+ model. Aided by the PPMI and ADNI datasets, this Multi-class Neurodegenerative Disease Dataset (MNDD) was generated. The outcomes of our experiments illustrate that the proposed model attains an exceptional accuracy of 99.27% on Dataset 1 and 99.14% on Dataset 2, surpassing the performance of several well-known existing deep learning models. Through advanced deep-learning techniques and image segmentation, this research improves early diagnosis and treatment outcomes in neurodegenerative disease classifications.

INDEX TERMS Neurodegenerative diseases, noise removal, data augmentation, CapsNet model, modified DenseNet-169 model, enhanced DeepLabV3+ model.

I. INTRODUCTION

The most commonly diagnosed neurological disorders in older adults are Parkinson's disease (PD) and Alzheimer's disease (AD) [1]. Alzheimer's disease frequently manifests as memory loss, difficulty performing daily duties, challenges with planning, etc. [2]. The leading cause of Alzheimer's disease and the disruption of normal brain cell activity is the decrease in some specific nerve cells together with neurofibrillary tangles [3]. Since AD is incurable, early detection will be crucial to patients receiving the proper care [4]. The most efficient method of diagnosing AD is by performing brain scans on the patient using CT, MRI, and PET images [5]. The disease is known as Parkinson's since James Parkinson was the first to describe it. Also frequently diagnosed with this PD are elderly individuals [6]. Parkinson's significant symptoms are low voice, shaky handwriting, sluggish motions, expressionless face, trouble

The associate editor coordinating the review of this manuscript and approving it for publication was Humaira Nisar.

© 2025 The Authors. This work is licensed under a Creative Commons Attribution 4.0 License.
For more information, see https://creativecommons.org/licenses/by/4.0/

getting up from a chair, stiff muscles, trembling, etc. [7]. PD is primarily caused by a dopamine shortage in the human brain, which results from neuron degeneration [8]. Similar to AD, PD is a highly progressing condition that is similarly incurable. Therefore, early diagnosis will be beneficial in ensuring that patients receive the correct care [9]. Compared to other medical imaging modalities, including PET, CT, etc., MRI scans are mostly favoured by doctors for diagnosing PD since they accurately display neuro-anatomic biomarkers [10]. Because these MRI scans are three-dimensional, the intrinsic intricacies of the subcortical structures captured in these MRI scans are complicated, even for radiologists, to analyze and interpret with the naked eye [11]. Therefore, developing an early screening system that can both support radiologists and conduct analyses while effortlessly managing the intricate features of these three-dimensional brain structures is essential [12].

Particularly in the last five years, the use of deep and machine learning techniques for classifying different brain anatomical abnormalities has shown to be particularly beneficial and research-oriented [13]. The machine learning-based CAD systems that use electronic medical records and imaging data are very accurate [14]. Much research has also been done recommending various CAD systems for automating the process of diagnosing lung, breast, and liver cancers, among other cancers, using CT, PET, fMRI, and MRI scans [15]. However, the amount of research conducted in the field of classifying neurodegenerative diseases is still significantly smaller than that of detecting glioma and other forms of brain tumors [16].

Due to their high performance and efficiency, researchers extensively utilize deep transfer learning models and conventional neural networks [17]. These deep learning models, like neural networks and deep transfer learning models, do not require human segmentation and feature extraction, unlike traditional machine learning models [18]. However, these conventional neural networks also tend to have certain flaws, particularly in pooling layers, which impact how well they function, particularly in image categorization tasks [19], [20]. For small, medium, and large image datasets, the Densenet-169 and DeepLabV3+ models are employed to overcome the shortcomings of the existing deep transfer learning and neural network models. Affine transformation and resilience to data rotations are two benefits of using DenseNet networks; however, they also demand tiny training datasets. Additionally, the DenseNet network-based models have produced excellent results in the areas of brain tumor, lung cancer, breast cancer, and other cancer-type classification. Image classification usually uses them to find the best weights for feature extraction and the capacity to deduce an image's spatial postural details; the DenseNet and DeepLabV3+ models perform better for the image classification tasks. The DenseNet-169 network is a perfect substitute for the multi-class categorization of neurodegenerative diseases because of all these qualities.

A. CONTRIBUTION

To increase the accuracy of diagnosing neurodegenerative diseases with brain MRIs, this research introduces a deep learning methodology. The following are the study's contributions:

- For the multi-class classification and segmentation of neurodegenerative diseases, a hybrid deep learning-based artificial intelligence system was introduced.
- To demonstrate the resilience, effectiveness, and relevance of this neurodegenerative disease model, training and testing of the proposed system uses a sizable MNDD dataset in real-time.
- With the model's ability to detect subtle brain changes and boost performance in neurodegenerative disease classification tasks, we have applied efficient pre-processing techniques such as noise filtering, contrast enhancement, and data augmentation.
- The disease-related useful features are successfully extracted using the CapsNet model to improve the proposed models' network performance, allowing the proposed model to achieve faster convergence and obtain greater accuracy.
- After feature extraction, the Modified DenseNet-169 model classifies the input MRI images into multi-class classification of neurodegenerative diseases.
- The accurate delineation of the affected region of neurodegenerative diseases is correctly segmented by the Enhanced DeepLabV3+ model.
- The Adam optimizer is conducted on several hyper-parameters of the proposed model to enhance its effectiveness and reduce the time complexity.
- The data is split into training and testing samples to validate the model. The simulation is conducted to test the model's efficiency, and the simulation results show higher accuracy than existing methods.

The research is divided into sections: Section II reviews the conventional segmentation and classification techniques associated with diagnosing neurodegenerative diseases. In Section III, the proposed methodology is clearly described together with functional details. The experimental outcomes of the proposed and conventional classification algorithms are assessed using various datasets and assessment metrics in Section IV. The paper's conclusion is reached with Section V's additional improvement.

II. LITERATURE SURVEY

This section reviews recent methods and algorithms for categorizing and segmenting neurodegenerative diseases. It also discusses the benefits and drawbacks of each technique used to classify brain diseases.

Alhudhaif [21] created a deep hybrid network using a CNN model and an ensemble classifier. Adapting the intense super-resolution neural network improves the MRI image's resolution. From the images, the features at both low and high levels were retrieved using the hybrid deep CNN. These

deep characteristics are then sent into the random subspace ensemble classifier based on the KNN classifier.

For PD classification, a new CNN model was introduced by Palakayala and Kuppusamy [22]. The model was created with extra attention and residual modules by fusing the LeNet and U-Net models (LUNet) for PD detection. Pre-processing and augmentation of the MR images were performed to enable accurate and effective deep-learning model training. Ahalya et al. [23] developed a new deep-learning model for PD classification. The DCGAN model is used for the data augmentation process. Pre-trained models like InceptionV3, Xception, and VGG16 were used for feature extraction and classification. The effective results are produced using the InceptionV3 model for feature extraction and the QSVM classifier for PD classification.

For AD classification, a deep learning-based multilayered framework was developed by Goyal et al. [24]. The binary and multi-class classifications use transfer learning-based LSTM and AlexNet models. For increasing the amount of the dataset, data augmentation techniques are employed after the images have been pre-processed using filtering procedures. Finally, an AlexNet model based on transfer learning is used to classify AD in many classes.

With a metaheuristic model, Devi and Raghavendran [25] suggested a novel deep learning-based model for segmenting and classifying MRI brain images to optimize the diagnosis of Alzheimer's disease. Initially, fuzzy Gaussian C-adaptive histogram equalization was used to collect and process the dataset for segmentation and noise removal. Particle Grey Wolf Firefly Optimization was then used to optimize the segmented image, and Support Vector Convolutional Graph Transfer VGG-16 learning was used for classification. A classification method incorporating uncertainty and spatial information was presented by Payares-Garcia et al. [26] to differentiate between patients and healthy individuals from four different neurodegenerative diseases. The feature extraction and classification tasks are performed using the SBNN model.

A unique structure-focused neurodegenerative CNN architecture called SNeurodCNN and an image brightness enhancement preprocessor employing gamma correction, two components of the deep learning system, was proposed by Odimayo et al. [27]. The focal structural atrophy features arising from the segmentation of brain regions collected by MRI are fed into the SNeurodCNN architecture. Consequently, the architecture uses regularization techniques to regularize learnable parameters and only considers the CNN components required to achieve the target classification job. These components consist of two fully connected layers and two down-sampling convolutional blocks. Table 1, summarizes the relevant literature on the classification of neurodegenerative diseases.

Noella and Priyadarshini [28] developed a generative adversarial Deep Convolutional Neural Network DCNN to diagnose the different types of dementia. The DCNN is used for feature learning and classification. This work concentrates on the three different types of dementia such as Alzheimer's disease (AD), Frontotemporal Dementia (FTD) and Parkinson's disease (PD). The designed model achieves an overall accuracy of 97.7% with 0.97- sensitivity and 0.97- specificity values. However, the DCNN model, a profound and complex architecture, requires substantial computational power and long training times.

A ranking-based ensemble approach was created by Goyal et al. [29] using the weighted strategy of deep learning classifiers. Three stages are included in the entire modelling process of the developed method. Since noise significantly impacts deep learning models' performance, pre-processing techniques are used in phase I to clean up and normalize datasets. In phase II, five deep learning models are chosen for classification and prediction result computation. After determining the ranks and weights of the five models, a ranking-based ensemble technique is developed in phase III to group the findings. Thus, the multi-class classification for the developed framework demonstrates a promising accuracy of 97.18% for AD and 97.85% for PD.

Existing models like Xception, InceptionV3, LSTM, RCNN, VGG, and ResNet cannot extract all the relevant features from complex brain images. With specific designs, the existing CNN models may find it easier to capture the fine-grained features of neurodegenerative diseases, frequently resulting in small changes in brain structure. This may result in incorrect categorization or inadequate segmentation of regions impacted by neurodegenerative changes, which are essential for precise diagnosis and medicinal planning.

Although neurodegenerative diseases frequently affect intricate, large-scale patterns in brain structures, most models concentrate on local feature extraction. This calls for a model that can represent the spatial relationships among various brain regions locally and globally. The lack of a model that can handle these spatial relationships effectively could lead to imprecise segmentation results.

The existing models are vulnerable to over-fitting when the dataset is small or more training examples must be needed. Neuroimaging data often have high dimensionality, which increases the risk of over-fitting. The robustness and generalization features of the model are affected by over-fitting, which results in poor performance on unseen data.

The small, subtle, or hard-to-detect regions of the brain that are essential for identifying neurodegenerative diseases, including early-stage Alzheimer's plaques or the shrinkage of particular brain regions in Parkinson's disease, were not well addressed by the majority of the earlier CNN-based models. Ignoring these regions can lead to incorrect or insufficient segmentation and misclassification, particularly in the early stages of the disease.

To address these difficulties, a new deep learning model is proposed by incorporating an attention mechanism, which helps the model focus on the most relevant regions and

TABLE 1. The summary of related prior works with advantages and disadvantages.

Reference	Year	Methods	Results	Advantages	Disadvantages
Alhudhaif et al. [21]	2024	KNN	Accuracy: 99.11% Sensitivity: 98.75% Specificity: 99.54% Precision: 98.65% F1-score: 98.70%	(i) It works well on tumors that are smaller in size. (ii) In neuroimaging data, KNN can spot anomalies or outliers pointing to uncommon or unusual neurodegenerative diseases.	(i) Both expensive and computationally demanding (ii) It is susceptible to noise in the data and unimportant features.
Palakayala et al [22]	2024	AttentionLUNet	Accuracy: 98.8% Sensitivity: 98.8% Specificity: 98.8% Precision: 98.8% F1-score: 98.8%	(i) It generates segmentation outputs of excellent quality. (ii) It handles and distinguishes complex, overlapping structures with effectiveness.	(i) Longer training periods and significant hardware resources are needed (ii) The two main problems were interpretability and over-fitting.
Ahalya et al [23]	2024	QSVM	Accuracy: 87.5% Precision: 95% Recall: 84% F1-score: 89%	(i) It reduces the complexity of the network (ii) The accuracy of the model is increased	(i) Its computational overhead is significant. (ii) Implementing and tuning QSVMs can be challenging and may require specialized knowledge and expertise
Goyal et al [24]	2024	Transfer learning based AlexNet model	Accuracy: 96.83% Sensitivity: 95.76% Specificity: 96.94%	(i) An appropriate and improved trade-off is produced by this model (ii) It produces high classification results	(i) The image quality directly impacts the CNN model's performance. (ii) It restricts its capacity to extract hierarchical patterns and intricate features from neuroimaging data
Devi et al [25]	2024	Support vector convolutional graph transfer VGG-16	Accuracy: 98% Precision: 95% Recall: 94% AUC: 90%	(i) It has a reasonable rate for categorizing images. (ii) It makes the network less complicated.	Need a proper feature extraction algorithm
Garcia et al. [26]	2023	SBNN	Accuracy: 83% Sensitivity: 85% Specificity: 81% F1-score: 82%	The model is designed to capture and employ significant anatomical features and patterns pertinent to precisely classifying diseases.	(i) High processing power is necessary. (ii) Redundant parameters resulting in issues with over-fitting
Odimayo et al. [27]	2024	SNeurodCNN	Accuracy: 98.1% Sensitivity: 99% Specificity: 97.2% Precision: 97.2% F1-score: 98.1%	(i) It manages multidimensional data efficiently. (ii) It generates an elevated level of categorization accuracy.	(i) Significant pre-processing methods are necessary (ii) When dealing with smaller datasets, there is a possibility of over-fitting.

features, ensuring better performance in classification and segmentation tasks.

A. PROBLEM STATEMENT

The research aimed to examine any anomalies in the brain's structure. The approach to features analysis and the methods for categorizing medical data images were also used to predict the research outcomes for efficiently identifying different neurodegenerative conditions. Based on the data, it is essential to diagnose Parkinson's and Alzheimer's disease since doing so allows for early detection and the continuation of the patients' treatment phases. Thus, during the diagnosis stage, the Quality MRI images were considered. However, this would show poorer spatial coverage, a longer scanning time, and a longer detection time while creating the qualitative images.

Every day, there is a notable increase in the MRI and biomedical processes. The brain MRI images are used to identify neurodegenerative diseases using hybridization approaches to segmentation and classification. Integrated DenseNet-169 and DeepLabV3+ models are used to classify and segment the affected regions of the input data based on these features.

III. PROPOSED METHODOLOGY

Radiologists can benefit from automated disease classification systems by having less work to do when starting treatment, which delays the progression of a disease and enhances the quality of life for patients. Over the past ten years, a paradigm shift in medical image analysis has occurred due to substantial advancements in machine learning and medical scanning. MRI in deep learning has gained popularity in computer-assisted systems due to its ability to extract high-level features through spatial invariance, local connection, and weight sharing. However, there are several significant research difficulties in the way of clinical application, and these issues serve as the basis for the contributions made throughout this research.

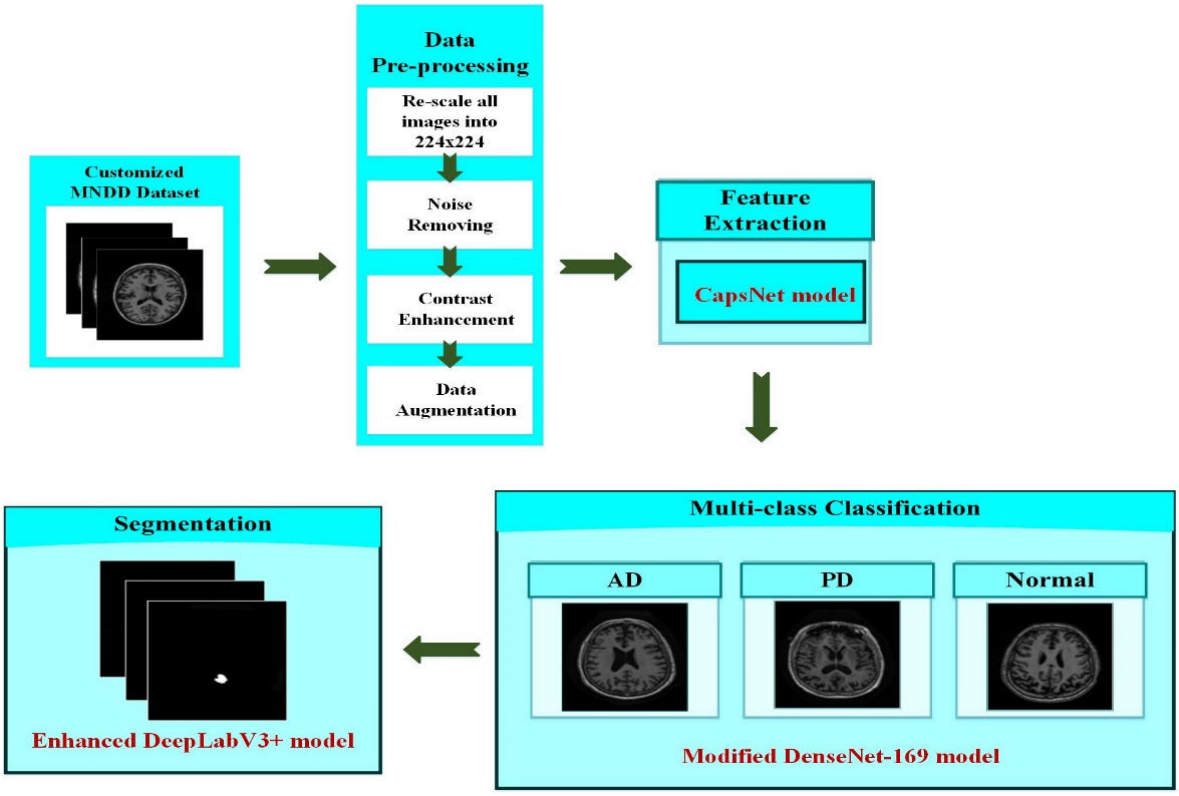

FIGURE 1. The architecture of a multi-class neurodegenerative disease diagnosis system.

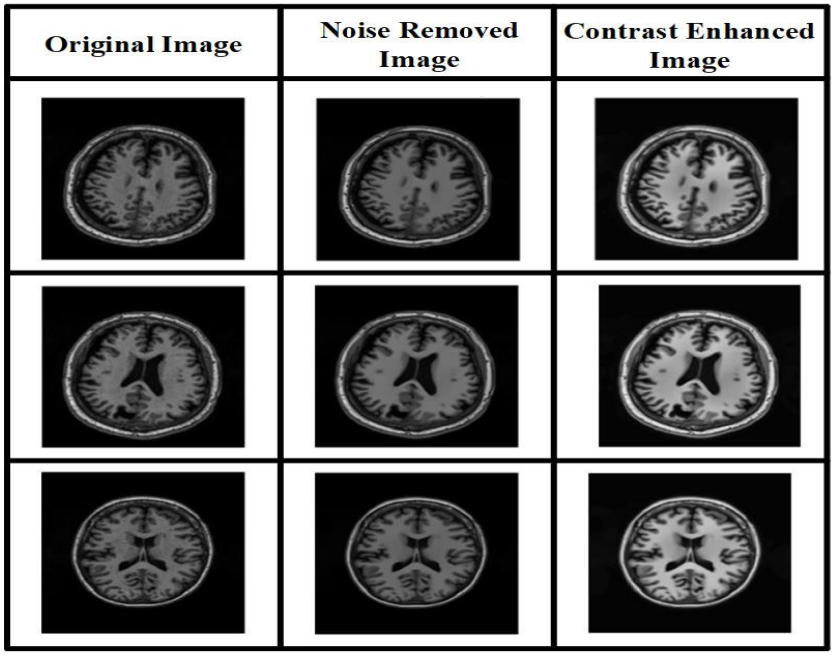

FIGURE 2. After pre-processing, the resulting images are shown in the first column, the coherent image is shown in the first column, images with noise reduced using NLM Filtering are shown in the second column, and the CLAHE output image is shown in the third column.

This research uses MRI and deep learning methods to create a framework for classifying neurodegenerative diseases. The stages of the proposed work are as follows, as seen in Figure 1. Pre-processing and augmentation of the MR images were performed to enable accurate and practical deep-learning model training. We employed the non-local means (NLM) filtering-based noise reduction method and a contrast-limited adaptive histogram equalization (CLAHE)

based contrast enhancement method to improve the quality and resolution of the images during the pre-processing stage. However, the deep learning models utilized in this research require a sizable training dataset to achieve better results. To enhance the classification findings and further address the over-fitting issue, this work also uses traditional data augmentation methods such as flipping, Gaussian blurring, scaling, and rotation. Following pre-processing, the CapsNet model is used to extract the disease-related features. The selected features are then fed into the Modified DenseNet-169 model for multi-class classifications of neurodegenerative diseases. To enhance classification performance in neurodegenerative disease tasks, we have adjusted the layer structure of the proposed DenseNet-169 classification model. This involves customizing the network to extract, process, and categorize disease-related data more effectively. Next, using the Enhanced DeepLabV3+ model, the region of interest from the categorized images is precisely segmented, resulting in a more precise delineation of the boundaries of essential brain regions afflicted by the disease. Utilizing the publicly examined MNDD dataset, the proposed approach's experiments are discussed. The model is validated by dividing the data into training and testing samples.

A. DATABASE DESCRIPTION

Two distinct sources provided this research's dataset: the PPMI and the ADNI databases. We have classified neurodegenerative diseases using two multi-class datasets based on publically available brain MRI images.

Dataset 1: The 2D axial images in this collection were taken from the ADNI baseline dataset. There are three categories of subjects: AD (Alzheimer's Disease), MCI (Mild Cognitive Impaired), and CN (Common Normal). The dataset has 1440 images of normal patients, 2590 images of MCI cases, and 1124 images of AD cases. The dataset images are collected from the Kaggle website (https://www.kaggle.com/datasets/katalniraj/adni-extracted-axial).

Dataset 2: The images in this dataset were taken from the PPMI and ADNI databases. There are three categories: normal (healthy) controls, AD, and PD. The dataset has 2500 images of AD cases, 2699 of normal cases, and 2391 of PD cases. The dataset images are collected from the Kaggle website (https://www.kaggle.com/datasets/toshall/neurodegenera tive-diseases).

B. DATA PRE-PROCESSING

This research uses the Multi-class Neurodegenerative Disease Dataset (MNDD), which gathers biology, imaging, and clinical data from several cohorts to identify markers of disease progression in neurodegenerative diseases. To increase the model's accuracy, we pre-process the MRI images in multiple phases before training the model. The dataset's images are first scaled to 224 × 224 pixels. NLM Filtering is used to eliminate the noise from the images. To improve image quality, we also pre-process brain MRI images using the CLAHE approach. We have used traditional data augmentation techniques to address the dataset's data imbalance issue, including Gaussian blur, rotation 90 degrees, up-down flipping, and left-right flipping. The sample of pre-processed images (noise-reduced and contrast-enhanced) is displayed in Figure 2.

1) NOISE REMOVING

NLM filtering functions differently from conventional local filters and effectively removes noise from brain MRI images. When searching for pixels with comparable intensity patterns, NLM filtering considers a broader image area than standard filters that only consider local pixel neighborhoods. Rician noise is one type of noise that is frequently present in MRI images and can be spatially connected. Because NLM filtering considers the global context and local intensity changes, it effectively addresses this type of noise. The NLM filter takes advantage of redundant data between patches in noisy images.

A non-local pixel's weighted average makes up each pixel in the filtered images. The equation $v(i) = u(i) + \eta(i)$ can be used to express image noise mathematically. At pixel i, the noise-free and noisy image pixels are described as $u(i)$ and $v(i)$ and the noise sample is depicted as $\eta(i)$. Throughout the entire image, the pixel value's weighted average can be used to determine the estimated pixel value $\hat{u}_{NLM}(i)$ by defining a search region, and it is described as,

$$\hat{u}_{NLM}(i) = \sum_{j \in S_i} w(i,j)\, v(j) \tag{1}$$

In the search domain S_i, the similarity between the pixels i and j determines the weight value $w(i,j)$.

2) CONTRAST ENHANCEMENT

Using CLAHE helps avoid excessive contrast amplification, which is essential to keep in mind while working with small areas of brain tumors in MRI scans. The reason for using CLAHE is that it operates at the tile level, which corresponds with the localized features of brain tumor locations in MRI images. To understand the mathematical foundations of CLAHE in the context of brain MRI scans, the procedure can be divided into several essential parts. The image is first split up into smaller areas, or tiles. The pixel intensity histogram for each tile is then calculated. The quantity of extreme value pixels is lowered by utilizing a contrast limiting function. The histogram inside each tile is then redistributed using histogram equalization. At last, the original image is recreated by combining the modified tiles. Equation 5 defines the contrast limiting function mathematically within CLAHE, where L is a constant that controls how much contrast is limited, the tile's lowest pixel intensity value is described as L, and the tile's highest pixel intensity value is represented as L_{max}.

$$f(x) = \begin{Bmatrix} 0, & if\ x < L \\ k\,(x - L)\,, & if\ L \le x \le L_{max} \\ k\,(L_{max}()) & if\ x > L_{max}\{\} \end{Bmatrix} \tag{2}$$

FIGURE 3. Results obtained by augmentation techniques.

However, by shifting pixel intensities, the visual contrast of the images is enhanced using histogram equalization. This is accomplished by mapping each pixel's intensity to a new value based on the cumulative distribution function of the image. As a result, the image's contrast is strengthened since its pixel intensities are distributed more uniformly. Rather than applying histogram equalization to the entire image, CLAHE does it uniquely within each image tile. This localized method preserves the local contrast features while preventing noise or other artifacts from amplified in the image. As a result, CLAHE generates an image that is sharper and has better contrast. CLAHE is essential for improving the contrast of medical images, such as the MRI images used in this research, because it highlights essential structures and details in the brain MRI images that would be difficult to see in other ways—the output images after pre-processing like filtering and contrast enhancement.

3) DATA AUGMENTATION

Using Gaussian blurring, flipping, scaling, and rotation techniques provides a workable way to increase the dataset's size without obtaining additional data. Applying these strategies can help guard against over-fitting, enhancing the model's ability to transfer knowledge to new, unobserved data. Data augmentation additionally strengthens the model's resistance to input image disparity differences, such as orientation, patient placement, or imaging settings.

First, in each scenario, we execute 50% probability flips from left to right and up to down. The image tensor is depicted as I, the flip of I horizontally is depicted as $I_1 flipped$, and the image width is described as W in equationequation (3) for up-down flipping.

$$I_{flipped(i,j,k)} = I\,(i, W - j - 1, k) \tag{3}$$

$$I_{flipped(i,j,k)} = I\,(H - i - 1, j, k) \tag{4}$$

We then rotate the input image by 90 degrees along any axis. In equation 5, the input image tensor is depicted as I, and the rotated version of I is described as $I_1 rotated$. The rotating 4×4 transformation matrix is an additional crucial component, which creates a new point (x', y', z') by rotating a point (x, y, z) around the z-axis by an angle theta. To revolve around another axis, the matrix must be adjusted correspondingly.

$$I_{rotated}\left(x', y', z'\right) = I\,(x, y, z) \tag{5}$$

TABLE 2. Data distribution both before and after data augmentation.

Datasets	Class	Before data augmentation	After data augmentation
Dataset 1	AD	1124	4496
	MCI	2590	5180
	CN	1440	4320
	Total	5154	13996
Dataset 2	AD	2500	5000
	Normal	2599	5398
	PD	2391	4782
	Total	7590	15180

TABLE 3. The data distribution for training and testing.

Datasets	Classes	Training (80%)	Testing (20%)
Dataset 1	AD	3597	899
	MCI	4144	1036
	CN	3456	864
Dataset 2	AD	4000	1000
	Normal	4318	1080
	PD	3826	956

In equation 6, the input image tensor is depicted as I, the Gaussian kernel is represented as k and B, as I's blurred version, is described as B for applying Gaussian blur as a data augmentation method. Figure 3 displays the result of these four augmentation processes. To improve deep learning models' functionality and generalization for medical image analysis, data augmentation is an essential approach. Table 2 displays the distribution of data following data augmentation.

$$I_{blurred[i,j,k]} = sum\,(sum\,(sum\,(k\,[x, y, z] * I\,[i - x, j - y, k - z]))) \tag{6}$$

C. DATA SPLITTING

A dataset containing MRI images of people with AD, PD, and healthy controls was used for our research. The publicly accessible dataset served as a valuable tool for our research. However, the dataset was divided into two subsets for our investigation, with 20% being utilized for testing and 80% for training. Interestingly, we only used our data augmentation techniques on the training set. The distribution of data following data augmentation is displayed in Table 3.

D. FEATURE EXTRACTION

The CapsNet model is utilized in this proposed method to extract the essential disease-related features and improve

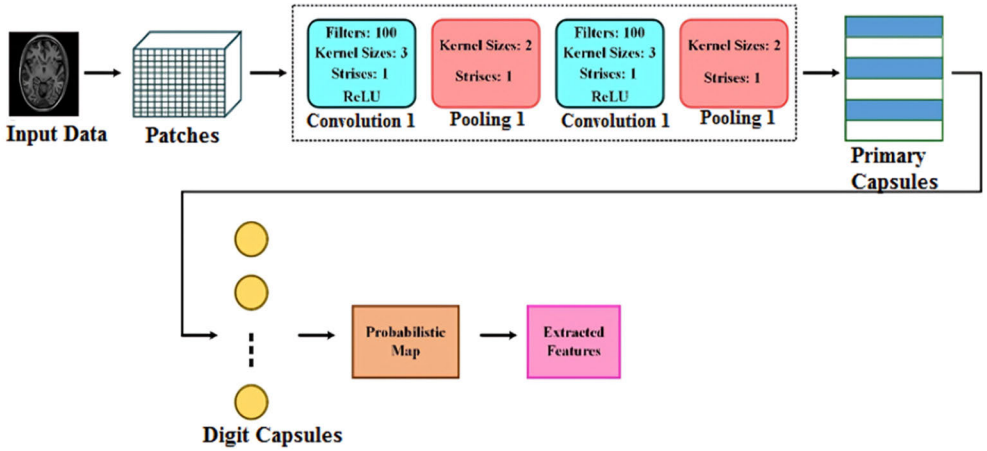

FIGURE 4. The CapsNet model structure.

classification performance. A neural network called CapsNet was recently proposed, and it has the potential to significantly affect deep learning, particularly in computer vision. The input and output of a neuron in a conventional CNN are scalars. In contrast, the vector is processed by the neurons in CapsNet. As a result, the capsule is also known as a vector neuron (VN), and a vector contains all of the essential data regarding the status of the features in the capsule detection process. Figure 4 displays the structure of the CapsNet model.

When deleting and resizing features, CNN pooling layers lose several essential features. Additionally, because a function that can get crucial data does not appear, a CNN cannot understand relationships among several eliminated features. CapsNet uses squash functions in combination with pooling layers. As a non-linear function that takes input using the vector method and resizes data in a vector of units without changing its alignment, this task will not cause any data to be lost. The following contains a measured formula for the capsule's operation,

$$\hat{u}_{j|i} = W_{ij} u_i \tag{7}$$

The prediction vector is denoted as $\hat{u}_{j|i}$, and it is accepted by capsule j and produced by capsule i; this multiplies the weight matrix W_{ij} by the output u_i of the capsule layer that came before it.

$$S_j = \sum_i c_{ij} \hat{u}_{j|i} \tag{8}$$

The total number of products $\hat{u}_{j|i}$ and c_{ij} produces results in s_j. In CapsNet, capsules were used in place of traditional CNN neurons, and each input and output unit was converted into a vector. The impacts of a particular unit on the input data are indicated by a vector orientation. An entity's potential existence in the current input is indicated by the magnitude of the capsule vector. The CNN activation function, or other ''squashing'' function, ensures that the vector length is between 0 and 1. Equation (9) can express the ''squashing'' function.

$$v_j = \frac{\|S\|}{1 + \|S\|^2} \frac{S_j}{\|S_j\|} \tag{9}$$

Concurrently, the capsule's entire input vector is depicted as S_j and the capsule j's output vector is depicted as v_j.

$$c_{ij} = \frac{exp\left(b_{ij}\right)}{\sum_j exp\left(b_{ij}\right)} \tag{10}$$

The dynamic routing model defines the coupling coefficient C in Equation (10). Its primary goal is to permit the input capsule to choose its path for broadcast to the next capsule layer. The softmax function is defined as c_{ij} and. It indicates the log prior prospect between capsules i and j. In previous layers, the Parameter b_{ij} is used by CapsNet to specify relationships between capsules i and j. In a layer, the coupling coefficient C comparable to entire capsules, and an early iteration b_{ij} is set to 0. Equations (11) were then used to update $\hat{u}$ and v_j. Using the dot product of v_j and $\hat{u}$, the following equation upgrades parameter b_{ij}:

$$b_{ij} = b_{ij} + \hat{u}_{j|i} v_j \tag{11}$$

The value of b_{ij} will increase after upgrading using equationequation (11) when the $\hat{u}_{j|i}$ and v_j dot product produces an optimistic result. By strengthening the bond between capsules i and j, Greater b_{ij} results in greater c_{ij}, producing greater S_j and v_j values. There will be harm to the link between capsules i and j if the dot product of v_j and $\hat{u}$ is negative.

E. CLASSIFICATION

This research effectively classified the multi-class classification of neurodegenerative diseases, including AD, PD, and normal cases, using a modified DenseNet-169 model.

One of the models in the DenseNet group, the Densenet-169 model, won the 2017 ImageNet competition. The feature maps in DenseNet relay the extra data collected from all previous layers to all ensuing layers. Information from levels above it is gathered by each layer. Since each layer receives feature maps from all previous layers, the network may be more constrained and narrow (and hence improves memory and computational efficiency). Even though it has more depth than other models, the DenseNet model has an

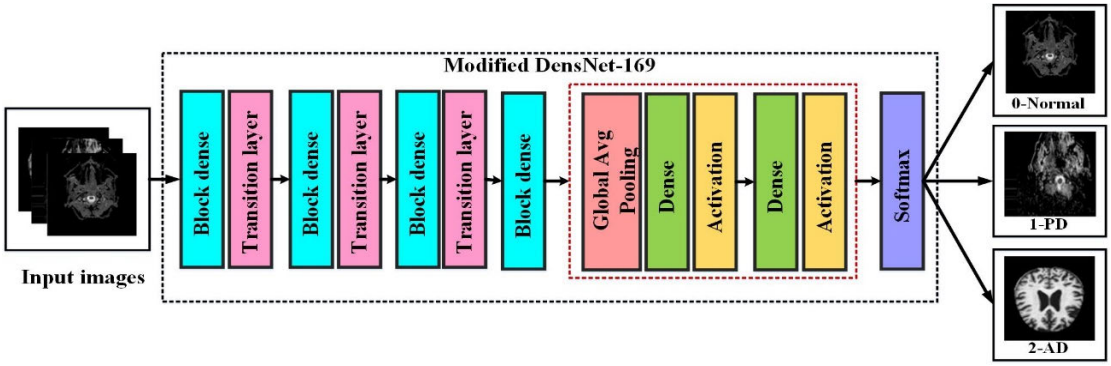

FIGURE 5. The structure of the modified DenseNet-169 model.

advantage because it has fewer parameters. Furthermore, the architecture successfully addresses the issue of vanishing gradients. Different variations of the DenseNet architecture, such as DenseNet-201, DenseNet-169, DenseNet-161, and DenseNet-121, have varying numbers of layers. We used the DenseNet-169 model in this research.

For image categorization, we modified the DenseNet-169 model. For a Global Average Pooling layer and two blocks, the Global Average Pooling layer and the two dense layers were specifically swapped out, each having an activation function and a dense layer. Figure 5 depicts the modified DenseNet-169 model structure; the red box denotes the model's modified layers. The SoftMax function is used to carry out the classification.

Overfitting may be more likely in the initial configuration with two dense layers, mainly if the dense layers are large. This can result in a model that matches the training data too closely and needs to perform better on fresh data. Dense layers typically include a large number of parameters. The vanishing gradient problem may worsen if several dense layers are used with no non-linearities between them, especially if the activation function needs to be appropriately selected. This may cause training to lag and make learning for the model more challenging. The model's memory consumption and computational cost are increased by two dense layers. This can be particularly challenging when dealing with large datasets or scarce hardware.

The model's capacity to capture non-linear correlations in the data is improved by adding blocks that combine dense layers with activation functions. The ReLU activation function introduces non-linearity, which helps the network select more intricate patterns. By adding activation functions between robust layers, the vanishing gradient problem can be mitigated, and more stable training can be made possible by maintaining the gradient flow during back-propagation. By including non-linear transformations in the feature extraction process with the help of these blocks, we can identify deeper patterns in the data and strengthen the model.

1) PARAMETERS OF THE PROPOSED MODIFIED DenseNet-169 MODEL

In our research, we used three activation functions. If the input is positive, the ReLU, and a piecewise non-linear or linear function, returns zero; if the input is negative, it produces the output immediately. ReLU is the activation function that neural networks frequently use, particularly CNNs and Multilayer Perceptrons. The definition of ReLU is mathematically expressed as:

$$f\ (x) = max\ (0, x) \tag{12}$$

SoftMax constantly maintains a value between 0 and 1, converting small or negative inputs into small probabilities and significant inputs into high probabilities. The SoftMax function can be described mathematically as:

$$\sigma\ (\vec{z})_i = \frac{e^{z_i}}{\sum_{j=1}^{k} e^{z_j}} \tag{13}$$

One mathematical function frequently utilized in neural networks is the Exponential Linear Unit (ELU) activation function. It is intended to get around the ReLU activation function's drawbacks, especially the ''dying ReLU'' problem.

We carefully considered the ELU and ReLU activation functions for hidden layer functions when creating the models we suggested. This decision was taken to mitigate the network's over-fitting risks. We utilized the SoftMax activation function for the output layer. Throughout 100 training epochs, the optimization process was carried out iteratively, allowing the models to improve their parameters gradually. A learning rate of 0.0001 was used throughout this procedure. A batch size of 32 was chosen to manage the data efficiently. The categorical cross-entropy loss function was used to calculate the difference between expected and actual results. This particular loss function works very well when there are several classes, like image classification tasks. The following equationequation expresses this loss function:

$$Loss = -\sum_{i=1}^{Outputsize} y_i . \log \hat{y}_i \tag{14}$$

The corresponding target value is depicted as y_i, and the output of the model's i^{th} scalar value is shown as $\hat{y}_i$. In the model's output, the number of scalar values is denoted by ''output size''. The Adam optimizer was chosen for the optimization process. This flexibility frequently results in faster convergence and better performance during optimization.

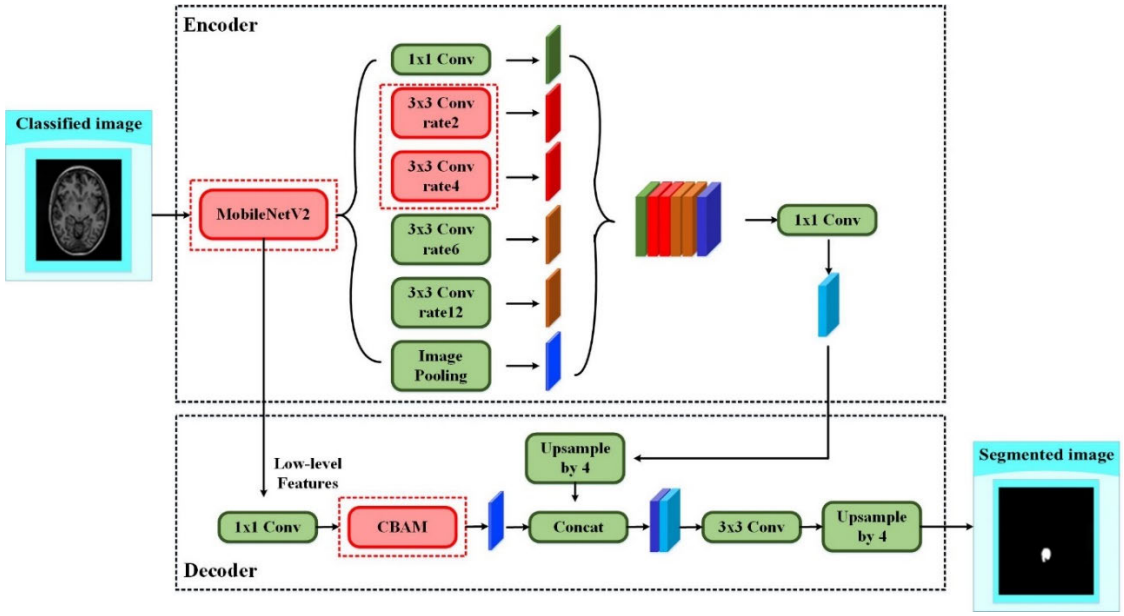

FIGURE 6. Enhanced DeepLabV3+ network structure.

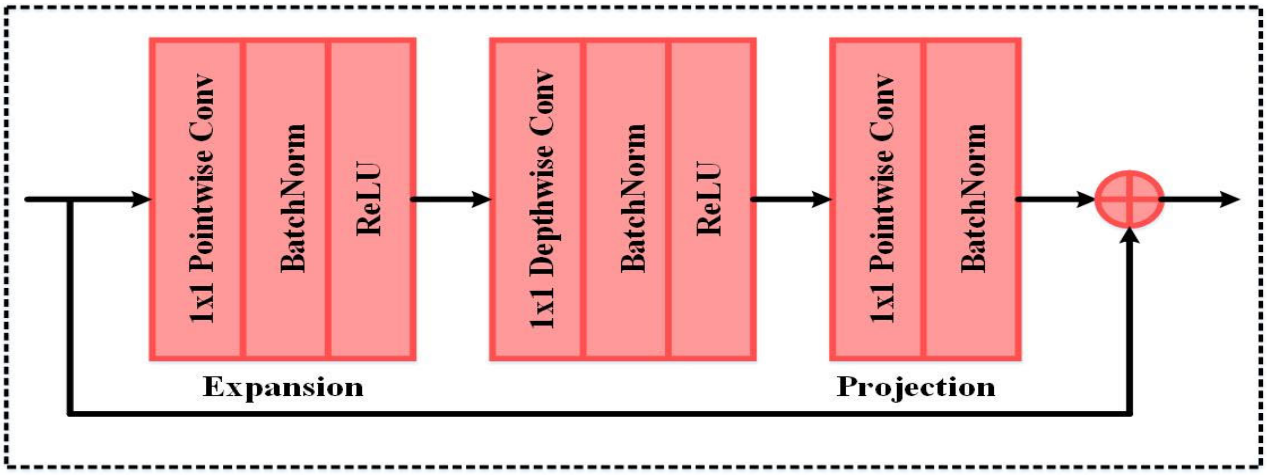

FIGURE 7. Network structure of MoblieNetV2.

F. SEGMENTATION

To precisely segment the disease region of the neurodegenerative diseases, the Enhanced DeepLabV3+ network model is used in the proposed research.

A deep learning network called the DeeplabV3+ model is tasked with semantically segmenting images. The encoder and decoder structures are maintained by the DeepLabV3+, but the network structure is optimized. To extract visual features, the network's encoding now includes the ASPP module with atrous convolution and Xception. The ASPP module executes various pooling operations at different scales on the image features to acquire the high-level features of the image. Then, after up-sampling, these high-level features are fed into the decoder, and the final feature representation is formed by fusing them with the low-level features. In addition to improving the model's comprehension of local and global information, the optimized structure can capture contextual details in the image at various scales, which helps mitigate the issue of feature loss and is advantageous when handling complex feature information in neurodegenerative disease segmentation.

The efficiency of the DeepLabV3+ network in refined feature categorization is limited by its complicated network structure and high computing resource requirements. However, it can combine multi-scale information and has excellent edge segmentation accuracy. To achieve the high-precision and high efficiency for brain tumor segmentation, this research modified and optimized the DeepLabV3+ network structure using MobileNetV2 as the backbone feature extraction network, changed the ASPP null rate, and added the attention mechanism convolutional block attention module (CBAM) in the decoding stage. Figure 6 shows the enhanced network structure of the DeepLabV3+ model. Model enhancements

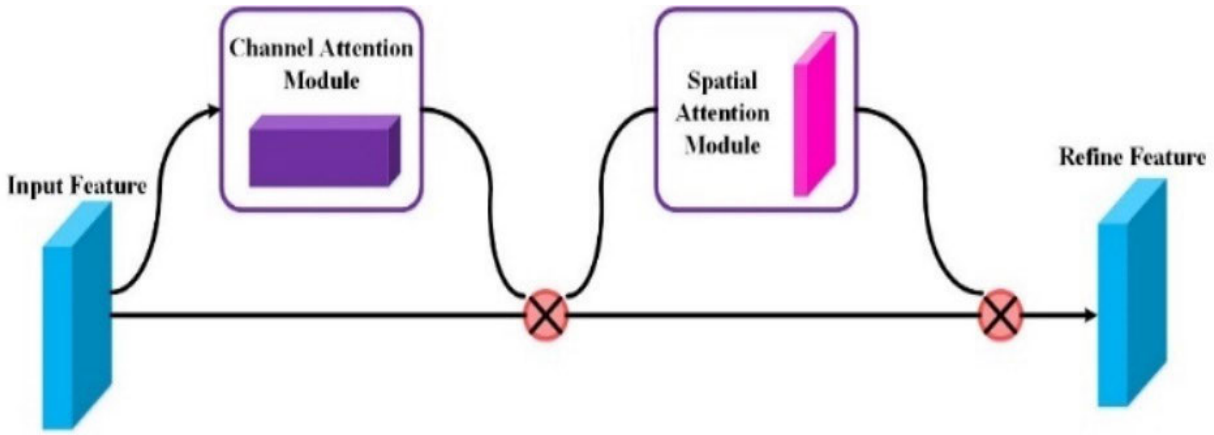

FIGURE 8. The structure of CBAM.

are demonstrated by the three boxes with dots in red.

1) REPLACE THE BACKBONE NETWORK

The DeepLabV3+ network usually uses Xception as its backbone network, which has the drawbacks of complicated network topology, lengthy training times, many parameters, etc. Google developed MobileNetV2, a simple CNN with rapid speed, moderate depth, and few parameters intended for embedded systems or mobile devices. Figure 7 illustrates its architecture. Three key components make up MobileNetV2: a linear bottleneck, inverted residuals, and depth-wise separable convolution. Compared to the conventional convolution procedure with the same amount of weights, the depth-wise separable convolution reduces computation by multiple scale orders. Before the 3×3 convolutional layer, the computation complexity is reduced by using the inverted residuals using 1×1 convolution and the dimensionality reduction is done by using the 1×1 convolution after the 3×3 convolution layer. The network can conduct feature expansion and feature compression due to the inverted residuals. The features are protected from being destroyed by the activation function by the linear bottleneck structure. It adds the residual network directly rather than using the activation function layer to reduce dimensionality. Improved feature compression and lightweight feature growth are possible with MobileNetV2. Thus, instead of using Xception as the main feature extraction network in this research, MobileNetV2 was used.

2) ADDING THE CBAM

Figure 8 illustrates the structure of the convolutional block attention module (CBAM), a deep learning attention mechanism module that improves convolutional neural networks' attention to significant features. The spatial and channel attention modules constitute the CBAM. To identify the connections between various channels and assign a weight to each channel's characteristics, the channel attention module is used to enhance concentration on the most significant channels. To better focus on significant spatial regions, finding the connections between different locations is the goal of the spatial attention module. It makes it easier for the module to concentrate on the task's spatially significant parts. For element-by-element multiplication, the channel and spatial attention module's outputs capture the connections between different weights and channels of the feature maps. By strengthening the network's capacity to recognize significant features, this combined attention mechanism enhances the model's performance. Consequently, the CBAM was incorporated into DeepLabV3+'s decoding stage in this research to focus on vegetation features from both the spatial and channel dimensions.

3) LOSS FUNCTION

Dice loss is the loss function utilized in training. The dice loss is considered information loss on both local and global scales. Dice loss, as shown in Equation 6 below, determines the number of positives and, by penalizing them, helps lower the number of false positives.

$$dice_loss = 1 - dice_score \tag{15}$$

For 20 epochs, early halting is utilized gradually to avoid the model over-fitting. During training, the model with the best metrics values is saved using the model checkpoint. With a learning rate 0.0001, Adam is the optimizer used to compile the model. Utilizing this optimizer has the advantage of being computationally efficient and requiring very little memory.

IV. RESULT AND DISCUSSION

This section enumerates all of the experiments carried out with the proposed approach and the assessment metrics. This section also includes the outcomes of the segmentation and classification processes. After these findings, we evaluate how well the proposed model performs compared to other cutting-edge models.

TABLE 4. Hyper-parameters for the proposed model.

S. No	Hyper-parameters	Modified DenseNet-169	Enhanced DeepLabV3+
1	Image size	224x224	224x224
2	Batch size	32	32
3	Number of epochs	100	100
4	Optimizer	Adam	Adam
5	Dropout rate	0.25	0.25
6	Learning rate	0.0001	0.0001
7	Activation function	Softmax, ReLU	Softmax, ReLU
8	Loss function	Categorical cross-entropy function	Dice loss function

A. SETUP CONFIGURATIONS

The proposed approach uses TensorFlow 2.7.0, CUDA 11.1, cuDNN, and Python 3.7.12 installed on Google Colab Pro1. The Colab Pro comes with 24 GB of RAM and T4 and P100 GPUs.

B. HYPER-PARAMETER TUNING

The best values for the proposed deep learning models are chosen in hyper-parameter tuning. These parameters are predetermined before the training starts; they are not learned from the data. Many parameters were considered for hyper-parameter tuning during the experiments, including learning rate, batch size, activation function, dropout rate, and epochs. The hyper-parameters for model training are listed in Table 4.

C. MODEL EVALUATION PARAMETERS

Extensive research of the proposed framework included a review of its accuracy, precision, recall, and F1 score. The precision of the model is assessed by minimizing the number of negative cases mistakenly classified as positive. On the other hand, recallrecall is a statistic that evaluates the model's accuracy in accurately classifying the right tumor type. An assessment statistic called the F1-score measures how well memory and precision are balanced. It is determined by multiplying recall and precision, dividing the result by their sum, and multiplying the result by two. This yields the harmonic mean of accuracy and recallrecall. Accuracy in the context of classification models quantifies the percentage of accurate classifications, which indicates the model's overall performance. It is computed by dividing the total number of predictions made by the number of correct predictions. The F1-score, recall, precision, and accuracy mathematical representations are shown in equations (16) – (19).

$$Precision = \frac{TP}{TP + FP} \tag{16}$$

$$Recall = \frac{TP}{TP + FN} \tag{17}$$

$$F1 - Score = 2 \times \frac{Recall \times Precision}{Recall + Precision} \tag{18}$$

$$Accuracy = \frac{TP + TN}{TP + TN + FP + FN} \tag{19}$$

The Intersection over Union (IoU) and Dice Similarity Coefficient (DSC) are two measures that are frequently used to assess how well image segmentation algorithms work. This research examined the segmentation model's (Enhanced DeepLabV3+) performance using DSC and IoU metrics.

The IoU metric measures how closely the expected and ground truth segmentation overlap are measured. It contrasts the two areas' union and overlap. Indicating the overlap between the predicted and ground truth segmentation, the Dice score calculates the similarity between the two sets. Compared to IoU, it is more sensitive to small objects.

$$IoU = \frac{|A \cap B|}{|A \cup B|} \tag{20}$$

$$DSC = \frac{2\,|A \cap B|}{|A| + |B|} \tag{21}$$

The predicted segmentation mask and ground truth segmentation mask are described as A and B. The values of IoU and DSC vary from 0 to 1, where 0 denotes no overlap and one perfect overlap.

To assess the effectiveness of the proposed network, we have also created confusion matrices, Receiver Operating Characteristics (ROC) curves, and Precision-Recall curves.

D. CLASSIFICATION RESULTS

Following pre-processing, 80% of the images are used for training and 20% for testing. Tables 5 and 6 present the classification report for neurodegenerative diseases using the proposed approach for Datasets 1 and 2. The proposed (Modified DenseNet-169) model for both datasets produced excellent precision values for each class. Compared to other classification models, the proposed disease diagnosis model produced fewer false positives and offered high precision values for the AD and PD classes. However, the precision value for the normal class is high since the disease screening model reduces false positives of a normal class. In Dataset 1, the disease screening model produced high recall values for the AD and normal classes. The proposed classification (Modified DenseNet-169) model for Dataset 1 achieves overall accuracy (99.27%), F1-score (99%), recallrecall (99.66%), and precision (99%). The proposed classification (Modified DenseNet-169) model for Dataset 2 achieves overall accuracy (99.14%), F1-score (99.33%), recallrecall (99.33%), and precision (99.33%). The visualization of the classified output images of Dataset 1 and Dataset 2 is shown in Figures 9 and 10.

E. SEGMENTATION RESULTS

With ground truth and expected masks, the proposed enhanced DeepLabV3+ segmentation model produces superior segmentation results. Only simpler tumor segments to categorize based on their morphology than those in other models are present in segmented images. Since normal classes don't include any tumor component, they have been ideally classified in predicted and ground truth

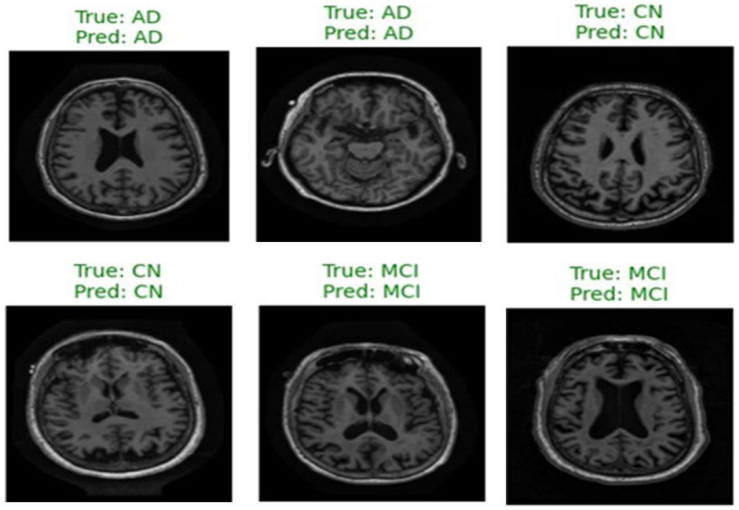

FIGURE 9. The classified output images of Dataset 1 using the proposed modified DenseNet-169 model.

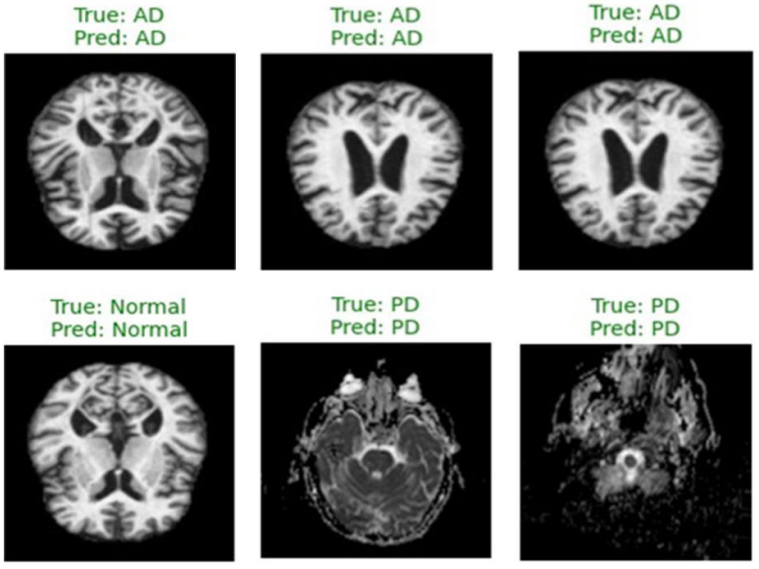

FIGURE 10. The classified output images of Dataset 2 using the proposed modified DenseNet-169 model.

TABLE 5. The classification report of Dataset 1 for multi-class neurodegenerative disease classification.

Validation Accuracy: 0.9927				
	Precision	**Recall**	**F1-Score**	**Support**
AD	0.97	1.00	0.98	929
CN	1.00	1.00	1.00	1139
MCI	1.00	0.99	0.99	2056
accuracy			0.99	4124
macro avg	0.99	1.00	0.99	4124
weighted avg	0.99	0.99	0.99	4124

TABLE 6. The classification report of Dataset 2 for multi-class neurodegenerative disease classification.

Validation Accuracy: 0.9914				
	Precision	**Recall**	**F1-Score**	**Support**
AD	0.98	1.00	0.99	1993
Normal	1.00	0.98	0.99	2160
PD	1.00	1.00	1.00	1919
accuracy			0.99	6072
macro avg	0.99	0.99	0.99	6072
weighted avg	0.99	0.99	0.99	6072

masks. However, several noises and artifacts are present in the published works for MRI image segmentation, which causes misclassification in the normal class of MRI images. Figure 11 displays the segmentation results of the proposed model for neurodegenerative diseases. The classified output images are shown in the first column, the ground truth images

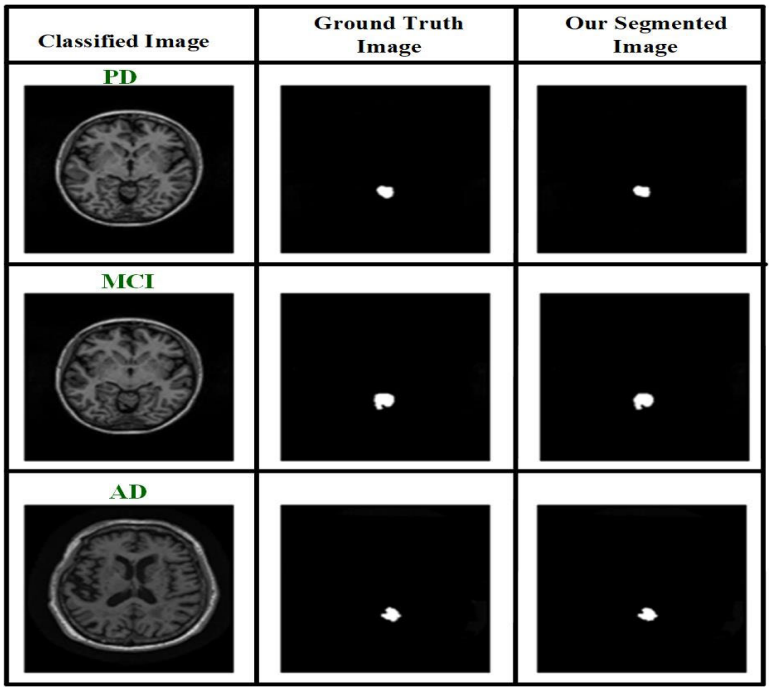

FIGURE 11. The segmentation outcomes of the proposed (enhanced DeepLabV3+) model.

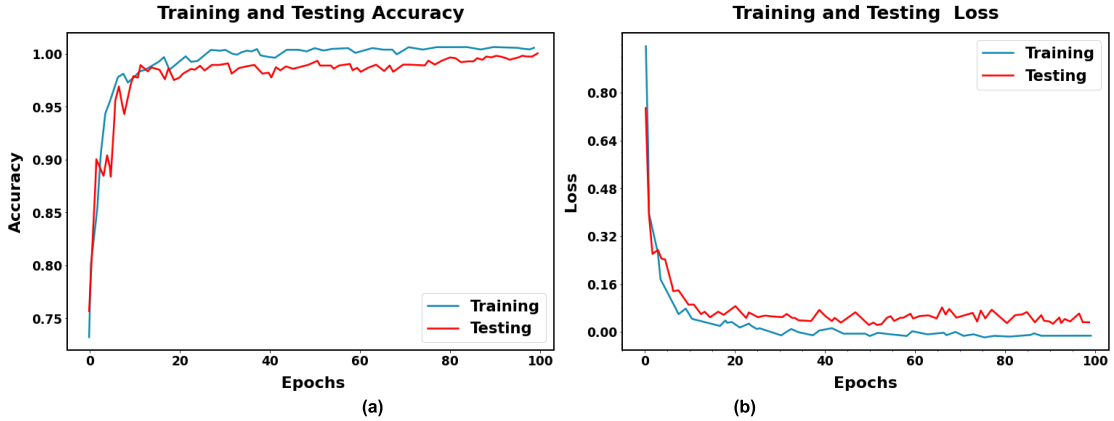

FIGURE 12. The (a) accuracy and (b) loss curves for training and testing using Dataset 1 in multi-class neurodegenerative disease classification.

in the second column, and our predicated segmented images in the third column. The proposed model segments the images with 98.57% IoU and 99.03% DSC measures for Dataset 1 and 98.25% IoU and 99.54% DSC measures for Dataset 2. The proposed methodology assists in differentiating between various neurodegenerative disease types by precise segmentation, which may result in more accurate and prompt diagnosis. Precise segmentation can help identify disease patterns specific to a patient, enabling more individualized treatments.

F. ACCURACY AND LOSS CURVES FOR TRAINING AND TESTING

Figures 12 and 13 display the proposed modified DenseNet-169 model's training and test accuracy-loss curves for Dataset 1 and Dataset 2. However, after just 20 training sessions, the model achieved over 99% training accuracy and 98% validation accuracy. The figure shows how, when the over-fitting problem is absent, the arc dramatically reduces the loss percentage during the training phase. The proposed model's predictions are better in line with the actual labels, as evidenced by its lower loss value for both datasets during training and testing. This is usually associated with better overall performance, ensuring the model learns well. In terms of good convergence, minimum training and testing losses with higher accuracy, the proposed model (Modified DenseNet-169) produced the best results.

G. ROC CURVE

The ROC curve visually represents a classification model's performance across several categorization parameters. The False Positive Rate (FPR) and the True Positive Rate (TPR)

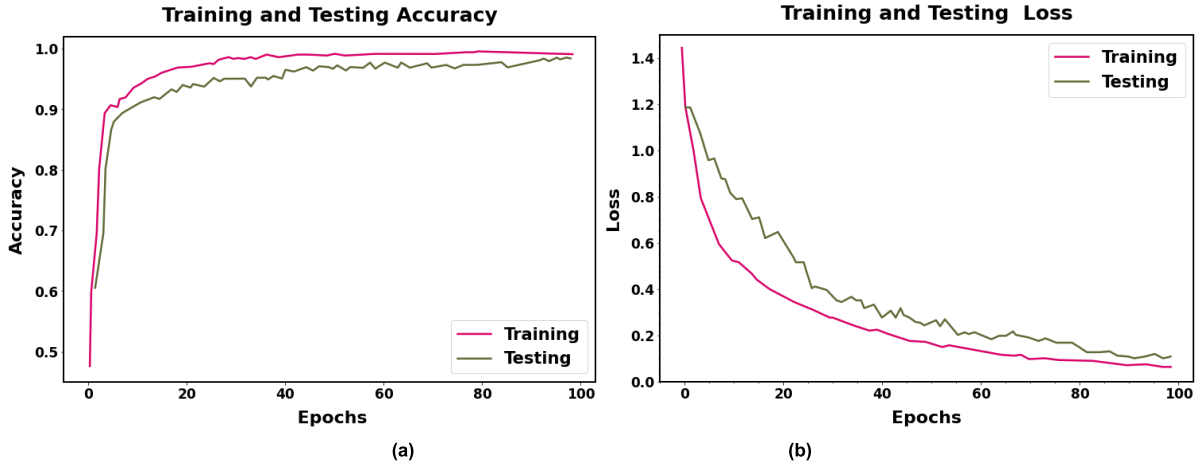

FIGURE 13. The (a) accuracy and (b) loss curves for training and testing using Dataset 2 in multi-class neurodegenerative disease classification.

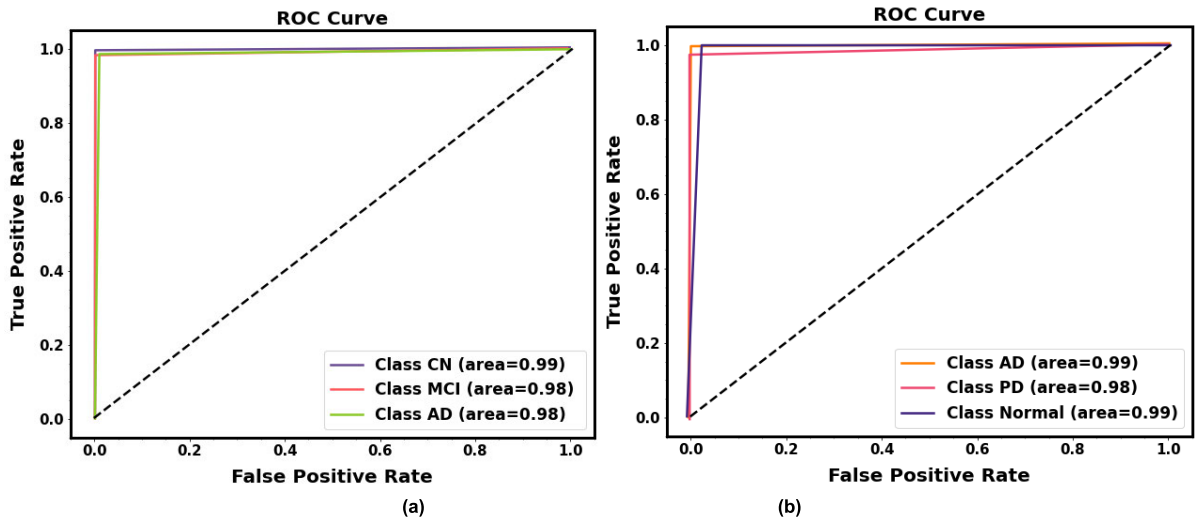

FIGURE 14. ROC curve for multi-class neurodegenerative disease classification for (a) Dataset 1 and (b) Dataset 2.

are shown graphically. The ROC curve balances correctly detecting positive occurrences and incorrectly categorizing negative examples as positive at each classification threshold in the testing set. The model's ability to differentiate between different thresholds is indicated by the ROC curve. For each of the three classes, the ROC curves for the test set utilizing Datasets 1 and 2 are shown in Figure 14. The AUC values are higher when ROC curves for all classes are contrasted with other currently used classification methods. For multi-class neurodegenerative disease classification, the proposed enhanced denseNet-169 model achieves an overall AUC (ROC) of 0.9833 for Dataset 1 and 0.9866 for Dataset 2. Because of its higher AUC values, our proposed model produces fewer false positives and negatives, improving its diagnostic efficacy.

H. PRECISION-RECALL CURVES

For multi-class neurodegenerative disease classification, the precision-recall curves for all the classes in Dataset 1 and Dataset 2 using the proposed method are shown in Figure 15. The proposed classification model produces higher precision and recall values (Modified DenseNet-169), ensuring that the model performs equally well in differentiating between normal, Parkinson's, and Alzheimer's cases and lowering the possibility of misclassifying one class for another. The proposed model works well despite class imbalances, indicating that it can detect diseases even when most of the dataset consists of normal cases, according to the high PR values (above 95%).

I. DICE COEFFICIENT AND DICE LOSS

While other segmentation approaches, such as UNet, UNet++, and Attention UNet, exhibited a more extensive range of values, the proposed Enhanced DeepLabV3+ model presented modest Dice and IoU values. The performance of dice score and dice loss curves for the proposed segmentation (Enhanced DeepLabV3+) model is shown in Figure 16. When comparing segmentation results amongst state-of-the-art algorithms, there are a lot of outliers. Compared to the other methods, the proposed approach produces relatively

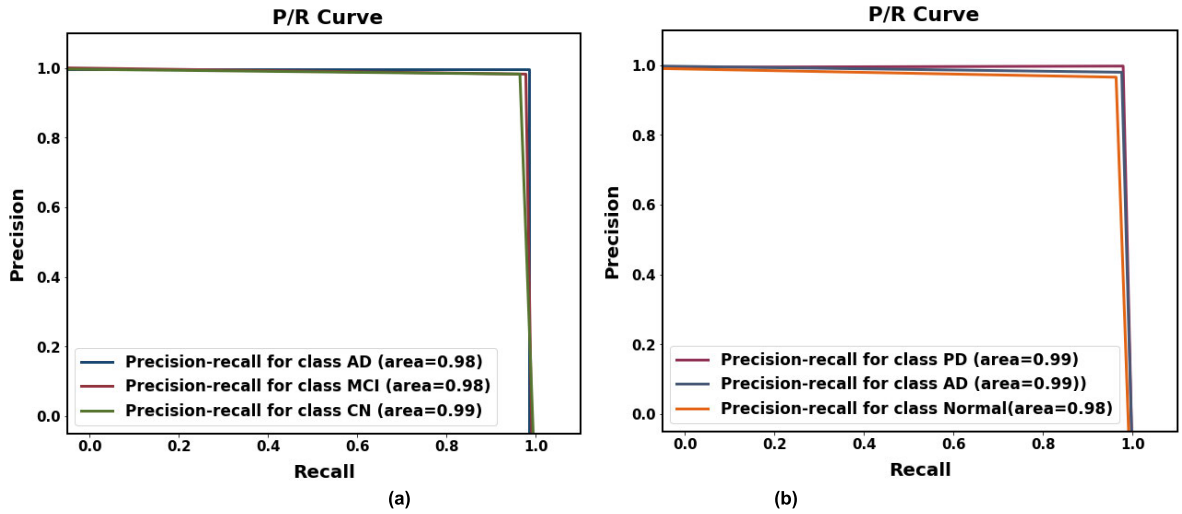

FIGURE 15. Precision-Recall curve for each class of neurodegenerative disease classification for (a) Dataset 1 and (b) Dataset 2.

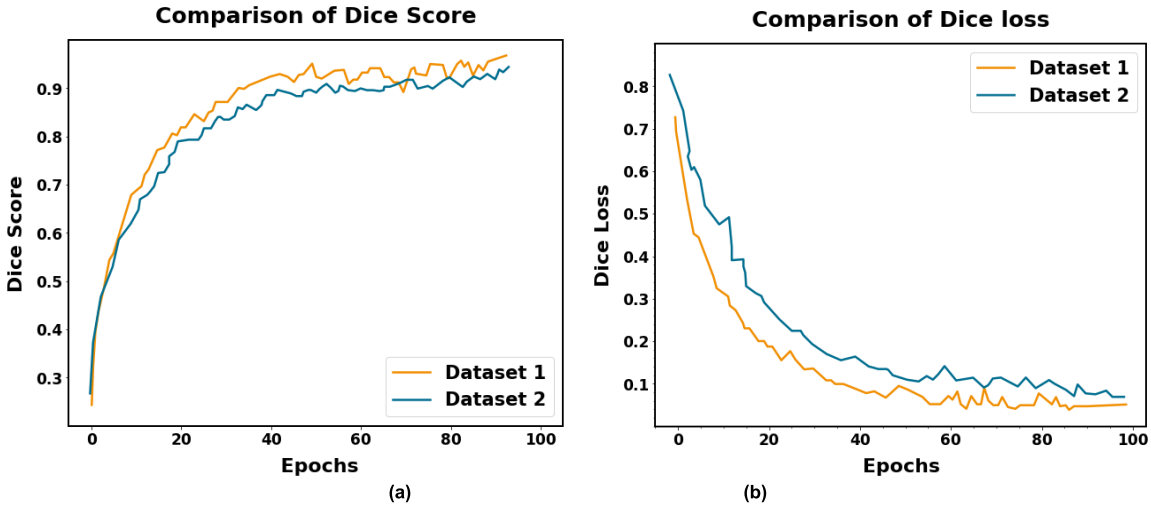

FIGURE 16. (a) Dice coefficient and (b) dice loss results for testing using the proposed segmentation (enhanced DeepLabV3+) model.

few outliers for the test samples. With a minimal dice loss and a high dice score, our Enhanced DeepLabV3+ model successfully segments the diseases. The boundaries of the regions of interest, such as lesions, atrophy, or aberrant structures associated with neurodegenerative diseases like Alzheimer's and Parkinson's disease, are being accurately captured by the proposed Enhanced DeepLabV3+ model. With a dice score of 99%, the proposed model successfully identifies smaller abnormal brain regions, which is helpful for early diagnosis and treatment planning. Robust segmentation across several patient datasets is provided by the Enhanced DeepLabV3+ model due to its potent feature extraction and multi-scale context capabilities, as well as its high Dice performance.

J. CONFUSION MATRIX

Figures 17 display the confusion matrix of the proposed model (Modified DenseNet-169) for classifying neurodegenerative diseases using Datasets 1 and 2. The proposed model performs well across all classes, as evidenced by the fact that it correctly identifies the most significant number of images in the provided datasets. The proposed model correctly classifies 860 images as normal, 892 as AD, and 1028 as MCI out of 2799 images in Dataset 1. The proposed model accurately classifies 1072 images as normal, 991 as AD, and 947 as PD out of 3036 images in Dataset 2. Based on confusion matrix results, the proposed model can manage complicated, multidimensional data and accurately distinguish between classes, lowering diagnostic errors and enhancing possible results. By improving the ability to distinguish various neurodegenerative diseases, the proposed Enhanced DenseNet-169 model lowers the probability of false positives and false negatives.

K. PERFORMANCE EVALUATION

Based on the classification performance, Table 7 compares the performance of the proposed model with that of different existing methods measured by F1-score, accuracy,

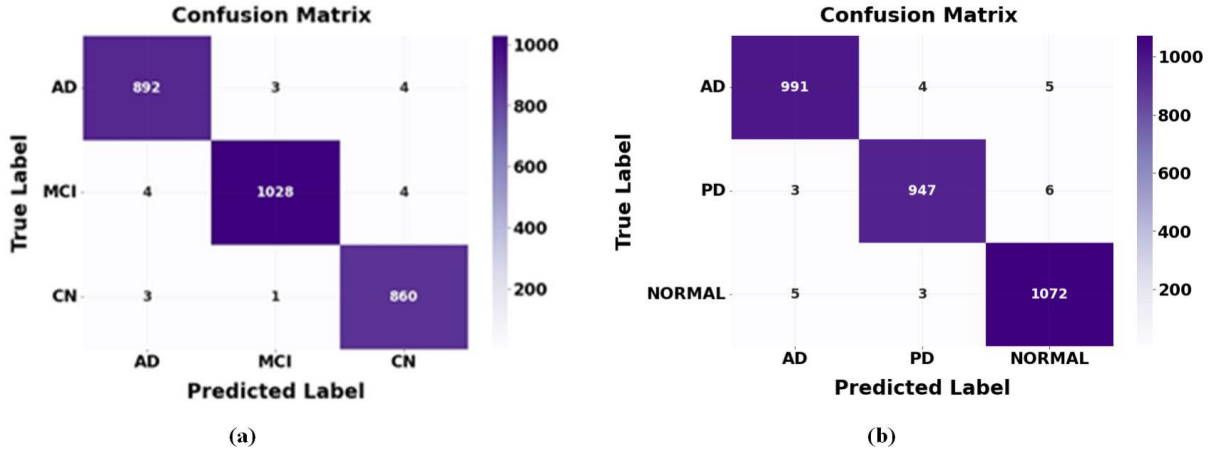

FIGURE 17. The confusion matrix of the proposed model (modified DenseNet-169) for (a) Dataset 1 and (b) Dataset.

precision, and recallrecall. Compared to cutting-edge techniques, our proposed classification model obtained the maximum accuracy of 99.27% for Dataset 1 and 99.14% for Dataset 2, demonstrating the higher quality of the model. When compared to existing deep learning models like AlexNet [30], SGCN [31], SBNN [26], DMANN [32] and machine learning models like KNN [28] and SVM [29], our proposed classification model (Modified DenseNet-169) model effectively classifies the neurodegenerative diseases with the precision of 99%, recall of 99.66%, and F1-score of 99% for Dataset 1 and precision of 99.33%, recall of 99.33%, and F1-score of 99.33% for Dataset 2.

Combining AlexNet with LSTM can lead to overfitting, especially with smaller or specialized datasets [24]. LSTM increases the model's parameter by adding sequential complexity that may not be required for spatial patterns in medical images. The DenseNet's dense blocks in our proposed Modified DenseNet-169 model minimize replicate learning and feature reuse, eliminating the requirement for many parameters. We have optimized the network using dropout and batch normalization approaches, which lowers the possibility of over-fitting.

The Bayesian inference needed to estimate uncertainties makes SBNNs [26] computationally demanding. Training and inference are slowed down by this process, which requires sampling and integrating across potential model parameters. By using dense connections to maximize deep feature extraction, DenseNet-169's architecture drastically lowers computational complexity when compared to SBNNs. DenseNet's dense connectivity allows for efficient feature propagation and reusability and extracting high-level spatial features directly from brain images, making it much faster to train and infer.

Our proposed Modified DesNet-169 model outperforms machine learning-based classifiers like KNN [30] and SVM [31] in handling high-dimensional data, capturing intricate spatial patterns, offering interpretability, and selecting important disease-related features. For the classification of neurodegenerative diseases, this leads to enhanced classification performance, robustness, and clinical relevance.

The depth and structural complexity of complex models like ResDesNet [32] can still cause problems in gradient flow, even though residual connections help mitigate gradient vanishing. This could impede learning in specific layers, especially when features need to be fine-tuned to detect changes specific to Alzheimer's disease. The Modified DenseNet-169 model prevents gradient vanishing and allows for efficient learning even in deeper layers because DenseNet-169's dense connections increase gradient flow without additional residual connections. This stability improves classification accuracy by capturing complex patterns specific to Alzheimer's and Parkinson's disease across all levels.

Compared to SGCN [34], the Modified DenseNet-169 features a more simplified architecture with fewer parameters and faster inference times. Because of this, it is more computationally efficient for processing large MRI datasets without the need for relational modelling's overhead or graph-construction stages, which are computationally costly in SGCN.

Learning disentangled representations across modalities is the model's goal. However, overlapping or redundant features could exist in single-modality or even limited-modal scenarios, which would lessen DMAAN's [35] efficacy. The model may need help concentrating on disease-specific features due to this overlap, which could lower classification performance. However, the interconnected layers of our proposed Modified DenseNet-169 model guarantee strong gradient flow and promote feature reuse, enabling it to learn intricate spatial information across all levels.

For neurodegenerative disease segmentation, the results of the proposed Enhanced DeepLabV3+ model and the comparative methods are described in Table 8. It is evident by examining this Table that the proposed Enhanced DeepLabV3+ model outperforms existing segmentation techniques in terms of segmentation results. The proposed model produced results on Dataset 1 of 0.9857 IOU, 0.9903 DSC, and Dataset

TABLE 7. The neuroimaging dataset's performance results using state-of-the-art techniques for multi-class neurodegenerative disease classification.

Reference	Year	Methods	Datasets	Accuracy (%)	Precision (%)	Recall (%)	F1-score (%)
Goyal et al [24]	2024	AlexNet-LSTM	Dataset 1	96.83	96.35	95.76	96.94
Garcia et al. [26]	2023	SBNN	Dataset 1	81.5	81	85	82
Selvaganesh et al [30]	2022	KNN	Dataset 1	98.6	99.21	95	96
Noella et al [31]	2023	SVM	Dataset 2	90.3	91.03	92.54	90.21
Hasan et al [32]	2024	ResDenseNet	Dataset 1	98	98.25	97.64	98.02
Alsharabi et al. [33]	2023	AlexNet–quantum learning model	Dataset 1	97	93	92	93
			Dataset 2	96	91.5	90	94
Zhou et al. [34]	2024	SGCN	Dataset 2	98.03	97.43	98.54	98.32
Wang et al [35]	2023	DMAAN	Dataset 2	98.26	98.04	98.63	98.64
Proposed Approach		Modified DenseNet-169	Dataset 1	99.27	99	99.66	99
			Dataset 2	99.14	99.33	99.33	99.33

2 of 0.9825 IOU, 0.9954 DSC. The region segmentation process in the existing deep learning models, including ResUNet, UNet++, UNet, and modified UNet, uses an exhaustive search strategy that is computationally demanding and takes a long time to process. Our proposed Enhanced DeepLabV3+ requires few parameters and minimal training time to segment the images.

In contrast to the UNet+ model [36], the CBAM in Enhanced DeepLabV3+ concentrates on certain spatial regions and channels, making disease-related features more effectively accessible. This attention process makes precise segmentation possible, particularly for small but essential diagnostic features. Because the proposed Enhanced DeepLabV3+ can integrate with an advanced loss function (Dice loss) and attention mechanism (CBAM), it is more resilient to class imbalance and changes in input data.

The effectiveness of the U-Graph Attention Network (GAT) Model [37] mostly depends on how well the graph generation procedure works, which is frequently done manually or using heuristic rules. Furthermore, GATs often experience over-smoothing, which makes it challenging to discern individual features in densely coupled graphs since node features converge. MRI scans' high-resolution spatial data. Instead of maintaining the fine spatial details necessary for accurate picture segmentation, the U-GAT model aggregates data across nodes, reducing the model's capacity to accurately segment brain regions impacted by disease. By explicitly highlighting significant spatial regions and feature channels, CBAM further refines features in the proposed Enhanced DeepLabV3+ model, strengthening the model's focus on brain regions relevant to disease.

Because RSS-DUNN [38] concentrates on smaller, specific regions, it may result in a fragmented understanding of the MRI image's larger context. Inaccurate segmentation may arise from an absence of contextual awareness, particularly when attempting to differentiate between healthy and diseased brain regions. Our Enhanced DeepLabV3+ uses ASPP, which applies various dilation rates to capture local and global contexts. This feature aids the model in identifying patterns specific to a given disease throughout the image.

Alzheimer's disease causes complicated anatomical variability by affecting different parts of the brain in various ways. Primary structural data can be captured by ResUNet [39], [41]. Still, it might not be as good at handling the anatomical variations in Alzheimer's disease, which call for deep learning models that can concurrently focus on global and local aspects. Our proposed DeepLabV3+ model adjusts the structural heterogeneity in Alzheimer's disease due to the combination of ASPP for global context and CBAM for dynamic attention in the proposed Enhanced DeepLabV3+ model. These modules enhance images' performance with intricate anatomical distinctions, resulting in more accurate segmentation, by dynamically adapting to various brain structures and disease changes.

L. DISCUSSION

This research proposed a deep learning method, the Modified DenseNet-169 model for neurodegenerative disease classification and the Enhanced DeepLabV3+ model for tumor region segmentation. When classifying neurodegenerative disorders into three types based on MRI images, the proposed Modified DenseNet-169 model outperformed other deep neural models regarding accuracy rate. This approach could help doctors diagnose brain tumors quickly and correctly. When compared to other studies that employed several methods, including machine learning classifiers like KNN, SVM, and RF and deep learning models like InceptionV3, AlexNet, SBNN, and SiameseNet, it was found that the Modified DenseNet-169 model is the most helpful method for categorizing multi-class neurodegenerative diseases. The proposed models' accuracy ranged from 99% to 99.30% across all classes, demonstrating the potency of deep learning methods in this field. It is important to remember, nevertheless, that caution should be used when assessing how well these models generalize to different datasets and clinical settings. Additionally, adaptable to various MRI classifications, the proposed method can be used in combination with transfer learning strategies to provide future classifications that are more accurate.

TABLE 8. Proposed performance comparison with state-of-the-art models for neurodegenerative disease segmentation.

Reference	Year	Methods	Datasets	IOU (%)	DSC (%)
Aparna et al [36]	2023	UNet+	Dataset 1	98.4	98.23
Hasan et al [37]	2024	U-GAT	Dataset 1	86.5	71.9
Palakayala et al [22]	2024	AttAggLUNet	Dataset 2	97.62	98.8
Gandhi et al. [38]	2022	RSS-DUNN	Dataset 2	73.6	81
Helaly et al. [39]	2022	RESU-Net	Dataset 1		94
Ganesan et al [40]	2024	Otsu thresholding method with TSA	Dataset 1	95	96
Rao et al [41]	2023	Deep ResUNet	Dataset 1	97.84	98.52
Proposed Approach		Enhanced DeepLabV3+	Dataset 1	98.57	99.03
			Dataset 2	98.25	99.54

Table 6's segmentation findings make it evident that, compared to standard UNet and other cutting-edge techniques like UNet++ and Attention UNet, the Enhanced DeepLabV3+ exhibits promising performance. Similarly, the Modified DenseNet-169 model outperformed the other existing methods in the classification task. Regarding AD tumors, nearly every segmentation model had comparable outcomes. This is so because the boundaries of benign tumors are usually spherical or curved in easily segmental patterns, and they lack fuzzy areas. However, due to their noisy nature and intricate forms, PD tumors are challenging to segment. Moreover, PD tumors spread quickly, making it difficult to define the limits of the tumor. Here, the Enhanced DeepLabV3+ model outperforms other cutting-edge techniques in performance. The segmentation findings demonstrate that the Enhanced DeepLabV3+ model outperforms the other models and produces an accurate segmentation mask, even for the most challenging tumor shapes. The encoder portion's DeepLabV3+ models assist in properly learning small, edge-sensitive malignant tumor boundaries. DeepLabV3+, in contrast to standard CNNs, minimizes information loss during down-sampling for shallow networks. The feature map's spatial dimension decreases due to the DeepLabV3+'s down-sampling. To solve this problem, a CBAM module is positioned between DeepLabV3+ and the decoder. It preserves the feature map's spatial dimensions while expanding its receptive field. As a result, compared to the other models, it produces better segmentation results. Plotting the dice score and loss versus the number of epochs results in two graphs. This graph shows that the proposed method's learning curve for Datasets 1 and 2 outperforms other models. DeepLabV3+'s sophisticated architecture improves the model's capacity to segment complicated brain components effectively.

M. ADVANTAGES

An extensive structure for research of neurodegenerative diseases is provided by combining Modified DenseNet-169 for classification with Enhanced DeepLabV3+ for segmentation. This combination offers both diagnostic and localization capabilities. This approach is useful for early diagnosis and monitoring the evolution of disease because it can identify and correctly classify small variations in brain structure. Dense connections between layers minimize the amount of parameters and over-fitting risk for classification. During back-propagation, the dense connections enhance gradient flow, guaranteeing consistent and effective training. The capacity of the proposed Modified DenseNet-169 model to extract intricate features allows for accurate classification of challenging multi-class issues, like distinguishing between AD, PD, and MCI. The DeepLabV3+ performs exceptionally well in semantic segmentation, accurately defining impacted areas (such as brain lesions or atrophied regions). By concentrating on the most pertinent spatial and channel-wise features, the Convolutional Block Attention Module (CBAM) improves feature representation and increases the accuracy of segmentation for small variations. The Enhanced DeepLabV3+ can manage the different lesion sizes and shapes found in neurological conditions because it uses atrous convolution to capture multi-scale contextual information.

N. LIMITATIONS AND FUTURE SCOPE

While the proposed CNN model for diagnosing brain tumors based on MRI images looks highly effective, there are significant limitations to consider. The accuracy and efficacy of the model might be restricted to the dataset used for training and validation. To guarantee its generalizability, the model must be tested on additional datasets and clinical settings. Another drawback of the proposed approach is that it might not be appropriate for categorizing different cancers or diseases. It is crucial to understand that the model may not work well for other medical image processing tasks because it was created and refined, especially for categorizing cerebral tumors from MRI images. Additionally, much data is required for the proposed CNN model to be adequately trained, just like any other deep-learning model. Smaller or lower-quality datasets might not allow the model to perform as well, even though it obtained excellent accuracy rates on the particular dataset employed. Furthermore, the model can be computationally expensive, which could restrict its usefulness in some situations.

In the future, we will collect a large, diverse dataset covering various cancers and diseases from multiple sources, enhancing the proposed model's adaptability across multiple medical image processing tasks. Additionally, we replace the standard convolutions with depth-wise separable

convolutions in the proposed models, which reduce the number of parameters and operations in each layer to reduce the computational complexity of the models.

V. CONCLUSION

The process of classifying various entities emerged as a challenging undertaking in the automation of brain tumor diagnosis. To address the shortcomings of the existing CNN networks, which have a high learning curve and computational complexity, this paper proposes hybrid deep learning models. MRI image pre-processing, segmentation, feature extraction, and classification are all part of the proposed model. Using an ensembled architecture of the Modified DenseNet-169 model with the Enhanced DeepLabV3+ model for MRI images, the distinctive neural network framework applies a multi-class classification and semantic segmentation model for pre-trained backbone networks. In the proposed research, the CapsNet model is used to extract the valuable features of the images. Then, the multiple neurodegenerative diseases are classified using the Modified DenseNet-169 model, and the classified images are properly segmented using the Enhanced DeepLabV3+ model. Two publicly available multi-class MRI image-based neurodegenerative disease datasets are used for experiment analysis. Our proposed method achieved the highest performance compared with other state-of-the-art methods. The proposed research achieves a classification accuracy of 99.27% for Dataset 1 and 99.14% for Dataset 2.

The proposed model is a potential tool in medical image analysis since its architecture is built for maximum performance on medical image datasets. It is imperative to acknowledge the constraints of the proposed model, including the necessity to thoroughly assess its applicability to alternative datasets and clinical situations and the possible expenses associated with computing and data needs. Future studies should concentrate on creating more reliable and accurate models by investigating different strategies and utilizing more, more varied datasets.

ACKNOWLEDGMENT

The authors declare that this manuscript is original, has not been published before, and is not currently being considered for publication elsewhere.

REFERENCES

[1] M. M. Hasan, J. Phu, A. Sowmya, E. Meijering, and M. Kalloniatis, "Artificial intelligence in the diagnosis of glaucoma and neurodegenerative diseases," *Clin. Experim. Optometry*, vol. 107, no. 2, pp. 130–146, Feb. 2024.

[2] R. A. Hazarika, D. Kandar, and A. K. Maji, "A novel machine learning based technique for classification of early-stage Alzheimer's disease using brain images," *Multimedia Tools Appl.*, vol. 83, no. 8, pp. 24277–24299, Aug. 2023.

[3] S. Agrawal and S. P. Sahu, "Image-based Parkinson disease detection using deep transfer learning and optimization algorithm," *Int. J. Inf. Technol.*, vol. 16, no. 2, pp. 871–879, Feb. 2024.

[4] Y. Dogan, "An innovative approach for Parkinson's disease diagnosis using CNN, NCA, and SVM," *Neural Comput. Appl.*, vol. 1, pp. 1–22, Nov. 2024.

[5] T. Prasath and V. Sumathi, "Pipelined deep learning architecture for the detection of Alzheimer's disease," *Biomed. Signal Process. Control*, vol. 87, Jan. 2024, Art. no. 105442.

[6] G. W. Jiji, "Biomarker to find neurodegenerative diseases using the structural changes in brain using computer vision," *Multimedia Tools Appl.*, vol. 82, no. 22, pp. 34981–34993, Sep. 2023.

[7] S. N. E. Toumi, N. Belkhamsa, Y. Cherfa, and A. C. Bouzouad, "An interpretable deep learning Bayesian optimized random forest framework for the diagnosis of Parkinson's disease in structural magnetic resonance images," *Int. J. Imag. Syst. Technol.*, vol. 34, no. 4, Jul. 2024, Art. no. e23106.

[8] M. K. Dharani and R. Thamilselvan, "Hybrid optimization enabled deep learning model for Parkinson's disease classification," *Imag. Sci. J.*, vol. 72, no. 2, pp. 167–182, Feb. 2024.

[9] A. Redolfi, S. De Francesco, C. Crema, D. Archetti, C. Muscio, M. J. Firbank, J. P. Taylor, and P. Tiraboschi, "Differential diagnosis of neurodegenerative diseases using an innovative deep learning approach," *Alzheimer's Dementia*, vol. 19, no. 1, 2023, Art. no. e06304.

[10] S. Asokan and A. Seshadri, "Hierarchical spatial feature-CNN employing grad-CAM for enhanced segmentation and classification in Alzheimer's and Parkinson's disease diagnosis via MRI," *Traitement du Signal*, vol. 40, no. 6, pp. 2769–2778, Dec. 2023.

[11] R. Souza, E. A. Stanley, M. Camacho, R. Camicioli, O. Monchi, Z. Ismail, M. Wilms, and N. D. Forkert, "A multi-center distributed learning approach for Parkinson's disease classification using the traveling model paradigm," *Frontiers Artif. Intell.*, vol. 7, Feb. 2024, Art. no. 130199.

[12] C. Choudhury, T. Goel, and M. Tanveer, "A coupled-GAN architecture to fuse MRI and PET image features for multi-stage classification of Alzheimer's disease," *Inf. Fusion*, vol. 109, Sep. 2024, Art. no. 102415.

[13] B. S. Rao, M. Aparna, S. S. Kolisetty, H. Janapana, and Y. V. Koteswararao, "Multi-class classification of Alzheimer's disease using deep learning and transfer learning on 3D MRI images," *Traitement du Signal*, vol. 41, no. 3, pp. 1–14, 2024.

[14] P. N. Kumar and L. P. Maguluri, "Deep learning-based classification of MRI images for early detection and staging of Alzheimer's disease," *Int. J. Adv. Comput. Sci. Appl.*, vol. 15, no. 5, p. 451, 2024.

[15] A. R. Palakayala, "Parkinson's disease classification based on enhanced ensemble learning and brain MRI," *Majlesi J. Electr. Eng.*, vol. 18, no. 1, pp. 1–13, 2024.

[16] Y. Tong, Z. Li, H. Huang, L. Gao, M. Xu, and Z. Hu, "Research of spatial context convolutional neural networks for early diagnosis of Alzheimer's disease," *J. Supercomput.*, vol. 80, no. 4, pp. 5279–5297, Mar. 2024.

[17] T. Samantaray, J. Saini, P. K. Pal, and C. N. Gupta, "Brain connectivity for subtypes of Parkinson's disease using structural MRI," *Biomed. Phys. Eng. Exp.*, vol. 10, no. 2, Mar. 2024, Art. no. 025012.

[18] A. Mehmood, F. Shahid, R. Khan, M. M. Ibrahim, and Z. Zheng, "Utilizing Siamese 4D-AlzNet and transfer learning to identify stages of Alzheimer's disease," *Neuroscience*, vol. 545, pp. 69–85, May 2024.

[19] S. Suchitra, L. Krishnasamy, and R. J. Poovaraghan, "A deep learning-based early Alzheimer's disease detection using magnetic resonance images," *Multimedia Tools Appl.*, vol. 1, pp. 1–22, Jun. 2024.

[20] J. Huang, L. Lin, F. Yu, X. He, W. Song, J. Lin, Z. Tang, K. Yuan, Y. Li, H. Huang, Z. Pei, W. Xian, and C. Yu-C. Chen, "Parkinson's severity diagnosis explainable model based on 3D multi-head attention residual network," *Comput. Biol. Med.*, vol. 170, Mar. 2024, Art. no. 107959.

[21] A. Alhudhaif, "A novel approach to recognition of Alzheimer's and Parkinson's diseases: Random subspace ensemble classifier based on deep hybrid features with a super-resolution image," *PeerJ Comput. Sci.*, vol. 10, p. e1862, Feb. 2024.

[22] A. R. Palakayala and P. Kuppusamy, "AttentionLUNet: A hybrid model for Parkinson's disease detection using MRI brain," *IEEE Access*, vol. 1, pp. 91752–91769, 2024.

[23] R. K. Ahalya, G. F. Nkondo, and U. Snekhalatha, "Automated detection of Parkinson's disease based on hybrid CNN and quantum machine learning techniques in MRI images," *Biomed. Eng., Appl., Basis Commun.*, vol. 36, no. 2, Apr. 2024, Art. no. 2450005.

[24] P. Goyal, R. Rani, and K. Singh, "A multilayered framework for diagnosis and classification of Alzheimer's disease using transfer learned Alexnet and LSTM," *Neural Comput. Appl.*, vol. 36, no. 7, pp. 3777–3801, Mar. 2024.

[25] T. S. Devi and V. Raghavendran, "MRI brain image-based segmentation and classification with optimization using metaheuristic deep learning model in Detection of Alzheimer's disease," *J. Comput. Anal. Appl. (JoCAAA)*, vol. 33, no. 2, pp. 154–169, 2024.
[26] D. Payares-Garcia, J. Mateu, and W. Schick, "Spatially informed Bayesian neural network for neurodegenerative diseases classification," *Statist. Med.*, vol. 42, no. 2, pp. 105–121, Jan. 2023.
[27] S. Odimayo, C. C. Olisah, and K. Mohammed, "Structure focused neurodegeneration convolutional neural network for modelling and classification of Alzheimer's disease," *Sci. Rep.*, vol. 14, no. 1, p. 15270, Jul. 2024.
[28] R. S. N. Noella and J. Priyadarshini, "Diagnosis of Alzheimer's, Parkinson's disease and frontotemporal dementia using a generative adversarial deep convolutional neural network," *Neural Comput. Appl.*, vol. 35, no. 3, pp. 2845–2854, Jan. 2023.
[29] P. Goyal, R. Rani, and K. Singh, "An efficient ranking-based ensembled multiclassifier for neurodegenerative diseases classification using deep learning," *J. Neural Transmiss.*, vol. 132, no. 1, pp. 67–93, Jan. 2025.
[30] B. Selvaganesh and R. Ganesan, "A hybrid segmentation and classification techniques for detecting the neurodegenerative disorder from brain magnetic resonance images," *Multimedia Tools Appl.*, vol. 81, no. 20, pp. 28801–28822, Aug. 2022.
[31] R. S. N. Noella and J. Priyadarshini, "Machine learning algorithms for the diagnosis of Alzheimer and Parkinson disease," *J. Med. Eng. Technol.*, vol. 47, no. 1, pp. 35–43, Jan. 2023.
[32] M. R. Hasan, A. B. M. A. Hossain, and S. M. A. Ullah, "Ensemble ResDenseNet: Alzheimer's disease staging from brain MRI using deep weighted ensemble transfer learning," *Int. J. Comput. Appl.*, vol. 46, no. 7, pp. 539–554, Jul. 2024.
[33] N. Alsharabi, T. Shahwar, A. U. Rehman, and Y. Alharbi, "Implementing magnetic resonance imaging brain disorder classification via AlexNet–Quantum learning," *Mathematics*, vol. 11, no. 2, p. 376, Jan. 2023.
[34] H. Zhou, L. He, B.Y. Chen, L. Shen, and Y. Zhang, "Multi-modal diagnosis of Alzheimer's disease using interpretable graph convolutional networks," *IEEE Trans. Med. Imag.*, vol. 1, no. 1, pp. 142–153, Jan. 2025.
[35] T. Wang, X. Chen, J. Zhang, Q. Feng, and M. Huang, "Deep multimodality-disentangled association analysis network for imaging genetics in neurodegenerative diseases," *Med. Image Anal.*, vol. 88, Aug. 2023, Art. no. 102842.
[36] M. Aparna and B. S. Rao, "Xception-Fractalnet: Hybrid deep learning based multi-class classification of Alzheimer's disease," *Comput., Mater. Continua*, vol. 74, no. 3, pp. 1–24, 2023.
[37] M. E. Hasan and A. Wagler, "A novel deep learning graph attention network for Alzheimer's disease image segmentation," *Healthcare Anal.*, vol. 5, 2024, Art. no. 100310.
[38] C. R. Gandhi and V. Murugesh, "Detection of neurodegenerative disease in brain using region splitting based segmentation with deep unsupervised neural networks," *Expert Syst.*, vol. 39, no. 6, Jul. 2022, Art. no. e12775.
[39] H.A. Helaly, M. Badawy, and A. Y. Haikal, "Toward deep MRI segmentation for Alzheimer's disease detection," *Neural Comput. Appl.*, vol. 34, no. 2, pp. 1047–1063, 2022.
[40] P. Ganesan, G. P. Ramesh, P. Falkowski-Gilski, and B. Falkowska-Gilska, "Detection of Alzheimer's disease using Otsu thresholding with tunicate swarm algorithm and deep belief network," *Frontiers Physiol.*, vol. 15, Jul. 2024, Art. no. 1380459.
[41] B. S. Rao, M. Aparna, J. Harikiran, and T. S. Reddy, "An effective Alzheimer's disease segmentation and classification using deep ResUnet and efficientnet," *J. Biomolecular Struct. Dyn.*, vol. 1, pp. 1–12, Dec. 2023.

SRINIVAS KATKAM received the Bachelor of Technology and Master of Technology degrees in computer science and engineering and the Ph.D. degree from Jawaharlal Nehru Technological University, Anantapur. He is working as a Professor and Head for the Department of Computer Science and Engineering (EA), Geethanjali College of Engineering and Technology. He is having 23 years of teaching background in various engineering institutes. He has been ratified as a Professor by JNTUH. He is a Philanthropist, Entrepreneur, Motivational Mentor, Profound Author, Publisher and Organiser of Technical Events. He published several books, research papers, technical reports and published five patents in his name. His research interests include artificial intelligence, machine learning, data structures, search engines, and data science.

V. PREMA TULASI received the M.Tech. degree from JNTUH. She is currently working as an Assistant Professor with the Department of Computer Science and Engineering (DATA SCIENCE), CMR Technical Campus (Autonomous). She served in academics for more than 13 years. Her multi-disciplinary research interests cover software engineering, computer networks, data science, artificial intelligence, machine learning, discrete mathematics, and software testing methodologies.

B. DHANALAXMI received the B.Tech. degree from CSIT, the M.Tech. degree in software engineering, and the Doctorate degree in computer science and engineering from JNTUH. She is currently working as an Associate Professor and HOD with the Department of Computer Science and Engineering - Cyber Security, Geethanjali College of Engineering and Technology, Hyderabad, Telangana, India. She has been with the Institute since 2021. She served in academics for more than 17 years. Her multi-disciplinary research interests cover software reliability, software engineering, computer networks, machine learning, data science, artificial intelligence, cryptography, and deep learning. As a Researcher she has filed ten patents, eight copyrights and more than 25 publications to her credit in different national and international journals including conference proceedings. She is a lifetime member of ISTE, IAENG, UACEE, and editorial board member of SCIREA.

J. HARIKIRAN received the Bachelor of Technology degree from JNTU Hyderabad, the M.Tech. degree from Andhra University, and the Ph.D. degree from JNTU Kakinada. He is currently working as a Professor with the School of Computer Science and Engineering, VIT-AP University, Amaravati, Andhra Pradesh. His research interests are microarray image analysis and hyper spectral image analysis. For more information, see harikiran.jhk@gmail.com.